A Computational Model based Study of Supervised Haptics-enabled Therapist-in-the-Loop Training for Upper-Limb Post-Stroke Robotic Rehabilitation *

Seyed Farokh Atashzar, *Student Member, IEEE*, Mahya Shahbazi, *Student Member, IEEE*,
Mahdi Tavakoli, *Member, IEEE*, Rajni V. Patel, *Life Fellow, IEEE*

Abstract—This paper proposes a new framework for neural-network-based supervised training of intensity and strategy for upper-limb haptics-enabled robotic neurorehabilitation systems for post-stroke motor disabilities. Two alternative approaches are implemented: (a) Haptics-enabled Teleoperated Supervised Training (HTST); and (b) EMG-based Indirect Supervised Training (EIST). The design of both techniques includes two phases: (a) characterizing and learning the therapeutic intensity and strategy when a therapist delivers robotics-assisted rehabilitation to a patient (demonstration phase), and (b) enabling regeneration of the learned therapeutic behavior when the therapist is out of the loop, e.g., when she/he is working with another patient (regeneration phase). For the first phase, HTST platform allows for *direct* transformation of the forces generated by the therapist to deliver rehabilitation at the patient side, and providing the therapist with *direct* force feedback. In contrast, EIST is an indirect platform which utilizes the posture of the therapist for generation of rehabilitation forces. EIST uses vibration to the therapist's arm to make the therapist aware of the forces applied to the patient's hand. Although HTST is a more intuitive alternative, EIST is safer, portable, wearable, less expensive, and provides relative motion freedom for the therapist. The proposed training framework is motivated by the existing challenge regarding the need for tuning the strategy and intensity of robotic rehabilitation systems in a patient-specific manner. It also enables therapists to share their time between several patients. Experimental results are presented to evaluate the engineering aspects of the work and feasibility of the concept, where a computational model is used to simulate motor disability of a post-stroke patient.

I. Preliminaries

Considering the increasing population of post-stroke patients, there is a need for increasing accessibility to rehabilitation therapies through the use of neuromechatronic technologies [1], [2], [3]. Programmable Virtual-Reality (VR)-based Haptics-enabled Robotic Rehabilitation (HRR) systems have shown great potential in accelerating Neural Plasticity (NP) and motor recovery for post-stroke patients [3], [4]. There are several factors which contribute to this effectiveness:

a) Robots are programmable and powerful and can be used for a wide range of patients with different biomechanics to deliver repetitive longitudinal motor therapy.

b) Robots can register motion and force profiles during therapies, which allows for accurate objective assessment.

c) VR-based environments provide patients with goal oriented tasks that enable them to use their decision-making abilities. This is a key factor for accelerating NP [2], [5].

Two forms of motor therapy have been commonly delivered by HRR systems: Assistive Therapy (AT), and Resistive Therapy (RT). AT is prescribed when patients cannot execute the required task. During AT, the robot guides patients while assisting them towards the correct path. RT is delivered when patients can manage to perform simple tasks. As a result, the robot may dissipate parts of the energy generated by the patients to make the task more challenging [2], [6].

In [7] and [8], comprehensive literature reviews have been presented on multi-modal stimulation of motor learning including haptics-enabled rehabilitation therapy. As discussed in [7], one of the open problems regarding the use of HRR technologies is the design of the assistive/resistive therapeutic force fields (called "therapy intensity" in this paper) to be delivered to the patient's impaired limb. This intensity is correlated to the choice of control parameters (such as the stiffness of the virtual guidance) considered for delivering haptic therapy. Although the control parameters are conventionally set as fixed values, it is believed that they need to be adaptively tuned by considering (a) specific kinematics and biomechanics of each patient, (b) the motor control capability of the patient, and (c) characteristics of neuromechanical deficits caused by the stroke [8]. It should be noted if more haptic guidance is delivered than needed, it can result in excessive reliance by the user on the guiding feedback. This can cause passive participation of the user instead of the interactive participation required to stimulate NP [7], [8]. Accordingly, automated adaptive techniques have been proposed in the literature to provide some level of adaptation considering the motor performance of the user [7], [8], [9], [10].

A. The Existing Challenge & The Motivation

Although using adaptive techniques, the performance of HRR systems can be improved, it is not possible to find an automated algorithm that matches the knowledge of a skilled therapist. In addition, although in general the literature supports the effectiveness of HRR systems, there are reports showing that in some cases, robotic therapy can be less effective than conventional manual therapy [11], [12]. It is believed that this observation is due to the lack of *flexibility* in tuning the control parameters compared to conventional therapy where the human therapist is capable of appropriately *modifying* the "strategy" and "amount of kinesthetic guidance" over the workspace [7], [8]. This modification of therapy by therapists is known to be a key factor for delivering effective therapy [13]. The challenge of appropriate and supervised tuning the therapeutic force generation by robotic systems in different parts of the workspace and for patients with different biomechanics provides the main motivation for this paper.

II. INTRODUCTION AND PROBLEM STATEMENT

Recently, machine learning techniques (such as those using probabilistic models) have been suggested for training robots based on demonstration performed by an expert [14]. This concept is tested for collaborative tasks [15], object manipulation tasks [16], [17] and for assistive technologies such as smart wheelchairs [18], [19] and cooperative assistive tasks [20].

In this paper, we propose a new framework that fuses the concepts of *machine learning* and *VR-based haptics-enabled assistive/resistive neurorehabilitation robotics* to address the challenges mentioned in Section I.A. The proposed framework has two major phases, namely (A) Supervised Therapy Demonstration (STD) phase, when the therapist is in the loop of interaction with the patient for delivering haptic rehabilitation, and (B) Regeneration through Modeling (RTM), when the therapist is not in the loop, for reproducing therapeutic behavior similar to that demonstrated in the first phase.

During the first phase (i.e., STD), the therapist controls the intensity and strategy of therapeutic force production. For this purpose, two different platforms i.e., EIST and HTST, are utilized which can enable keeping the therapist in the loop of robotic rehabilitation. In the next phase (i.e., RTM), the distribution of the therapeutic intensity/strategy are modeled using a Neural Network (NN) algorithm. The learned kinesthetic behavior of the therapist will then be regenerated for the patient while the therapist can use his/her time to work with another patient. These steps can be repeated as many time as needed and the therapist can change the strategy repetitively. This architecture is an alternative to tuning the intensity and strategy of the therapy and brings back the *conventionally-absent* kinesthetic supervision of a human therapist during robotic therapy (the challenge that is mentioned in Section I.A). Another outcome of the framework is a new visualization technique that can provide a heat map of the intensity of the delivered therapy by the therapist for each session. The map can be used by clinicians for monitoring progress of a patient over several sessions of therapy. The schematic of the proposed framework is shown in Fig. 1(a). In Fig. 1(a), HTST and EIST are the platforms (introduced below), using which (a) the kinesthetic therapy is generated by the therapist and is delivered to the patient while the therapeutic behavior of the therapist is registered; and (b) proper real-time feedback is provided to make the therapist aware of the forces being applied on the patient's limb. The therapist uses force information to decide about the sensorimotor needs of the patient. The two platforms are described below:

A) Haptics-enabled Teleoperated Supervised Training (HTST): This platform is a telerobotic system, whose feasibility and implementation were studied recently by the authors [21], [22], [23], [24]. The system is composed of two force-enabled robotic devices, one at the therapist's side and the other at the patient's side. The control algorithm provides virtual viscoelastic coupling between the motions of the therapist and those of the patient. This architecture allows the therapist to (a) directly tune the intensity and strategy of therapy, and (b) directly receive kinesthetic forces that brings the therapist awareness of the forces applied to the patient.
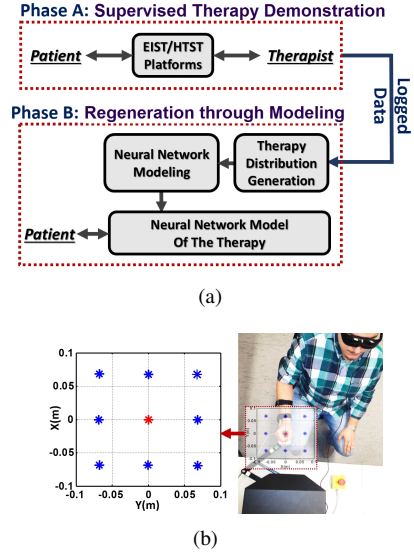
Fig. 1. (a) Schematic diagram of the Proposed Framework. (b) The workspace of the robot that corresponds to the VR environment.

B) EMG-based Indirect Supervised Training (EIST): This is a new platform proposed in this paper, which is composed of two wearable wireless armbands to be used by the therapist. The armbands can measure EMG activities of the therapist for detecting his/her posture to be used for tuning the strategy and intensity of the therapy (as explained later). In addition, the armbands can provide vibrotactile cues to the arms of the therapist. The EIST platform does not enable *direct* kinesthetic awareness for the therapist during the STD phase. Instead the architecture provides vibrotactile feedback for the therapist which brings him indirect awareness of the forces applied to the patient's hand. The indirect haptic awareness used here is motivated by the literature on *sensory substitution* used for telerobotic surgical systems (e.g., [25], [26]). Although, indirect force feedback is not as intuitive and informative as direct kinesthetic feedback realized by HTST, there are specific benefits with the use of EIST such as (a) lower cost, (b) guaranteed stability due to elimination of the need for closed-loop force feedback, and (c) better portability. The EIST platform still allows to keep the therapist in the loop of robotic rehabilitation and makes it possible for the therapist to tune the strategy and intensity of the therapy in real-time based on awareness of the forces applied to the patient's hand.

Remark 1. In the design of both EIST and HTST platforms a VR environment is used which is shared between the therapist and the patient. Two different objects (e.g., two circles) in VR are assigned to the motions of the therapist and those of the patient. The motion of the patient is measured by the robot and is mapped to the corresponding object. For HTST, the motion of the robot on the therapist's side is also measured and mapped to the corresponding object while in the EIST platform, the posture of the therapist is used. The above-mentioned two objects are coupled using a virtual viscoelastic band. As a result, the therapist can change the characteristics of the forces applied to the patient's hand (amplitude and direction) by moving (changing the position of) the object assigned to him/her. In fact, the therapist can assist the patient by leading his/her motion towards the target in the shared VR environment, or can resist the patient's movements thus,
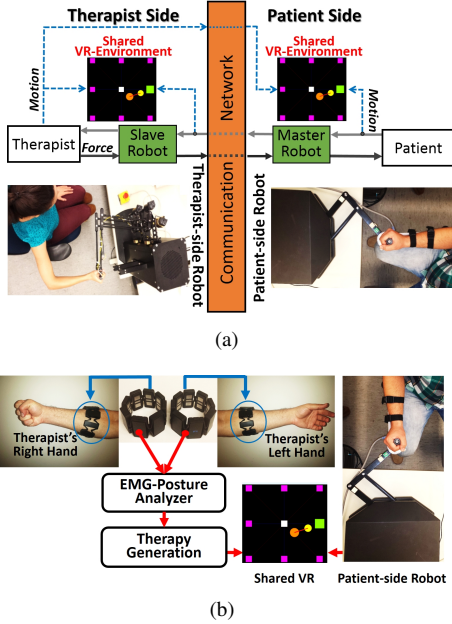
Fig. 2. (a) A schematic of the implemented HTST platform. The VR environment is shared between the therapist and the patient where the orange and yellow circles correspond to the patient's and therapist's movements respectively. The red line is the virtual viscoelastic coupling. (b) A schematic of the implemented EIST platform. The therapist-side system composed of two EMG armbands from Thalamic Labs Inc. which measure the muscle activity of the therapist's hand and provides vibrotactile cues.

changing the therapy strategy. With the proposed viscoelastic coupling, the patient is allowed to make mistakes in tracking the target while performing motor tasks. This is an important factor for motor learning [7], as opposed to rigidly controlling the patient's motions. The intensity of the therapy can be tuned by the therapist based on the distance between his/her position and that of the patient in the shared VR. The schematics of the implemented platforms are shown in Fig. 2 . ●

Remark 2. The Major contributions of this paper:
1) Designing a new neural-network-based therapy-regeneration-through-demonstration *framework* to learn the kinesthetic supervision of a therapist in the loop of robotic rehabilitation and replicate this behavior for longer periods when the therapist is not in the loop. The work is motivated by extending the time of exposure to interactive robotic therapies for patients, while minimizing the time during which the therapist should be directly involved with the patient; and maximizing the use of the time of therapists by modeling their kinesthetic supervision over the therapy delivered during a session. The proposed framework is implemented on two *platforms* (EIST and HTST).
2) Designing a new platform (i.e., EIST) using which a therapist can tune the strategy and intensity of robotic therapy while receiving vibration feedback according to the forces applied to the patient's limb. In addition to EIST, the HTST platform is suggested to register the intentions of a therapist. EIST is designed in this paper, while HTST is a subcategory of a more general technology that was recently developed by the authors [21], [22], [27]. Both platforms fuse the advantages of using HRR systems and having a therapist in the loop. The common goal is to provide patients with an "augmented" therapeutic environment that incorporates the therapist's expertise instead of conventional "virtual" therapy. ●

III. METHOD

In this section, the design of the proposed framework is described. As mentioned earlier, the framework consists of two separate phases STD, and RTM. STD is conducted using the two different platforms, namely HTST and EIST, while the second phase is the same for both platforms.

A. Phase A: Supervised Therapy Demonstration

During the first phase, the therapist provides rehabilitation and tunes the intensity and strategy of therapy based on her/his knowledge regarding the needs of the patient. For this purpose, two alternative platforms are proposed, as explained below.

Platform #1: Haptics-enabled Teleoperated Supervised Training: The first platform is a haptics-enabled telerobotic system that enables the therapist to directly interact with the patient and feel the kinesthetics of rehabilitation during task performance. In other words, this platform can provide the therapist with direct haptic awareness of interaction. A Two-channel Haptics-enabled Architecture (THA) [22] is considered to design the telerobotic architecture. For this, the patient is placed at the conventionally-called "master" console of the telerobotic system, where she/he can provide the required motion to perform a task in the shared VR environment. The therapist is placed at the "slave" console where she/he can feel the motions generated by the patient and can provide forces to be reflected back to and felt by the patient.

Modeling: To investigate the performance, first, the haptic interaction models at the therapist's side and the patient's side are explained. The patient-robot haptic interaction model is:

$$\delta_m(t) * v_p(t) = u_{cm}(t) + f_p(t). \tag{1}$$

In (1), $\delta_m(t)$ is the impulse response of the linearized model of the master robot, $*$ is the convolution operator, $u_{cm}(t)$ is the control input to deliver the therapy (the design of $u_{cm}(t)$ is explained later), $v_p(t)$ is the patient's hand velocity, and $f_p(t)$ is the force applied by the patient to robot. The force felt by the patient $f_p^r(t)$ is in the opposite direction to $f_p(t)$, so $f_p^r(t) = -f_p(t)$. For $f_p(t)$, we have the following decomposition:

$$f_p(t) = f_p^*(t) - \zeta_p(v_p, t). \tag{2}$$

In (2), $f_p^*(t)$ is the voluntary component of the force applied by the patient to perform the task and $\zeta_p(v_p, t)$ is the non-linear reactive component of the force which results from the biomechanical response of the patient's hand to the movement applied by the robot. Similar to the above, the therapist-robot haptic interaction model can be described by

$$\begin{aligned} \delta_s(t) * v_{th}(t) &= u_{cs}(t) + f_{th}(t), \\ f_{th}(t) &= f_{th}^*(t) + z_{th}(v_{th}(t), t). \end{aligned} \tag{3}$$

In (3), $\delta_s(t)$ is the impulse response of the linearized model of the slave robot, $u_{cs}(t)$ is the control input (the design of $u_{cs}(t)$ is explained later), $v_{th}(t)$ is the therapist's hand velocity, and $f_{th}(t)$ is the force applied by the therapist to the slave robot to administer the therapy. In addition, $z_{th}(v_{th}(t), t)$ denotes the nonlinear reaction dynamics of the therapist's hand and f_{th}^* is the exogenous force applied by the therapist to generate the haptic therapeutic response based on the patient's need.

Visoelastic Coupling: After developing the local models, control signals $u_{cm}(t)$ and $u_{cs}(t)$ should be designed to complete the telerobotic loop and generate the viscoelastic coupling between the therapist's and the patient's movements. The proposed designs are explained below. A block-diagram of the closed-loop telerobotic system can be seen in Fig. 3(a).

$$u_{cm}(t) = c_1(t) * v_p(t) + \hat{f}_{th}(t) \quad where \ c_1(t) = \delta_m(t); \quad (4)$$

$$u_{cs}(t) = -\gamma(t) * (\hat{v}_p(t) - v_{th}(t)) + c_2(t) * \hat{v}_p(t) \\ where \quad c_2(t) = \delta_s(t). \quad (5)$$

In (4) and (5), $\hat{f}_{th}(s)$ is the therapeutic force, received at the patient's side; and $\hat{v}_p(t)$ is the patient's hand velocity, received at the therapist's side. In this paper, particular attention is paid to the design of $\gamma(t)$. In fact, $\gamma(t)$ makes the mentioned viscoelastic coupling. Note that $\gamma(t) = \mathscr{L}^{-1}[\Gamma(s)]$, where $\mathscr{L}(\cdot)$ denotes the Laplace transform, and $\Gamma(s)$ is designed as

$$\Gamma(s) = \Delta_s(s) - \frac{K_v + \theta_v \ s}{s} \ where \ \Delta_s(s) = \mathscr{L}[\delta_s(t)]. \quad (6)$$

In (6), K_v is the stiffness constant and θ_v is the viscosity constant of the viscoelastic coupling provided by the proposed telerobotic system between the motions of the patient and those of the therapist. To clarify how this design generates viscoelastic coupling, we combine (1) to (6). The result is:

$$F_p^r(s) = \hat{F}_{th}(s); \\ F_{th}(s) = (K_v + \theta_v \ s) \cdot (P_{th}(s) - \hat{P}_p(s)). \quad (7)$$

The first equation in (7) states that the force felt by the patient, $F_p^r(s)$, is equal to the force generated by the therapist, $F_{th}(s)$. The second equation indicates that the therapeutic force, $F_{th}(s)$, is the output of the viscoelastic dynamics $(K_v + \theta_v \ s)$ where the stiffness and viscous parameters are K_v, θ_v. The input signal to the dynamics is the position error, $P_{th}(s) - \hat{P}_p(s)$, generated by the therapist between his/her movements and those of the patient. Thus, the therapist can assist or resist the patient's movement by providing various error profiles. The HTST system gives both users the feel of haptic interaction through the coupling. Allowing the therapist to directly feel the coupling forces enables haptic awareness for him/her.

Remark 3. Considering (7), the therapist can stretch the software-generated viscoelastic coupling to produce higher forces. In other words, the therapist can change $P_{th}(s)$ that results in changing the intensity of the therapy by modifying the magnitude of the position error (i.e., $P_{th}(s) - \hat{P}_p(s)$). Also, the therapist can change the strategy (assistive versus resistive) by changing the direction (sign) of the error. This error-based therapist-in-the-loop force generation approach that uses the viscoelastic coupling between the therapist and the patient is used in both HTST and EIST platforms. The design is motivated by the accepted need for providing freedom during interaction to accommodate motor learning [7].●

Platform #2: EMG-based Indirect Supervised Training: The second platform is a new architecture which can also keep the therapist in the loop of robotic rehabilitation. It is proposed to log the therapist's intention in changing the intensity and strategy of therapy through the therapist's hand posture. Using this indirect strategy, the therapist is mainly free to move his/her hand and body because the therapist can tune the therapy by distinct or continuous posture-based inputs (not movement-based inputs). In this paper, the *fist posture* is considered as the posture of interest. The platform is shown in Fig. 2(b). The utilized armband and an example of one out of eight available EMG readings are shown in Fig. 3(b).

Two EMG armbands are utilized in the implemented EIST platform. The use of the wearable wireless armbands provides movement freedom for the therapist. This (portability) is one advantage of the EIST system over HTST. As mentioned, the EIST platform is not capable of providing the therapist with direct kinesthetic awareness. Instead, vibrotactile feedback is provided according to the amount of force applied to the patient's hand to indirectly make the therapist aware of the forces. The sensory substitution, is not as intuitive as directly reflecting back the kinesthetic forces, but it eliminates concerns regarding stability and safety of a closed-loop telerobotic rehabilitation architecture [21], [27]. In addition, currently each armband costs about US $ 200. Consequently, at the therapist's side the EIST setup costs about US $ 400. However, the cost of having a second robot (considering the workspace and the required forces), can be several orders of magnitude higher. As a result, the design of the EIST system is cost-effective which is an advantage of this platform over HTST.

To implement the EIST platform, a three-step protocol is designed. The goal of the first step is to collect enough data which is then used in the second step to learn (for detection) the posture of interest to be used in the third step. The third step maps the detected posture of interest to the intended therapy which will then be provided to the patient using the rehabilitation robot. The steps are described below.

Step #1) The therapist wears the two EMG armbands below his/her elbow joints. There is no need for accurate placement of the armbands. The therapist will be asked to perform the following postures: (a) waving out, (b) waving in, (c) expanding fingers, (d) making a fist, and (e) four finger-to-thumb touching postures. The postures are shown in Fig. 3(c). In this protocol, each one of the postures needs to be kept for 5 seconds while having 2 seconds rest in between. The posture of interest should be kept for 15 seconds. The setup is equipped with a binary foot pedal. The pedal needs to be pushed by the therapist during the posture of interest. As mentioned, we chose the *making fist* posture to register the therapist's intention for tuning the therapy. The output of the pedal is a binary value that is used to distinguish the posture of interest from other postures. This value is "1" during the posture of interest and is "0" during other postures. This procedure forms step #1 of the protocol and the time needed to run this step is about 1 minute for each arm (i.e., 2 minutes in total). ●

Step #2) The goal of the second step is to find a mapping between the 8-dimensional space of the EMG measurements (provided by each armband) and the 1-dimensional space of the detected posture of interest (given by the foot pedal). The mapping is named *EMG Analyzer*. The EMG Analyzer should have high sensitivity to the specified posture of interest and close-to-zero sensitivity to all other postures. Based on our observations and to find an appropriate mapping, we considered the history of measurements and some dynamical features as well. For this purpose, two digital low-pass filters
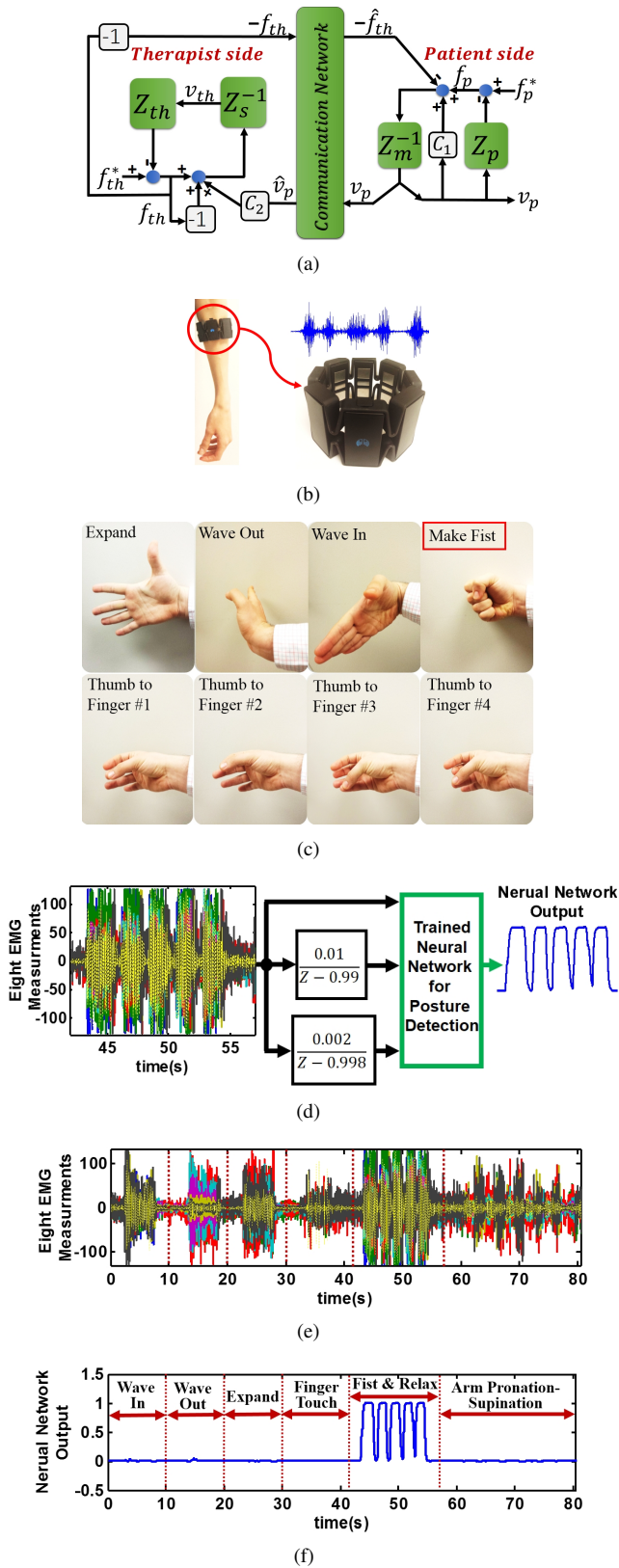
Fig. 3. (a) Block diagram of the HTST system ($Z_m(s)$, $Z_s(s)$, $Z_{th}(s)$, $Z_p(s)$ are Laplace transformations of δ_m, δ_s, ζ_p and z_{th} respectivelu). (b) Placement of the the EMG armband (from Thalamic Labs Inc., Canada) and a sample of the recording during the fist-and-relax task. (c) Calibrating Postures. (d) The neural network used and the corresponding inputs and output. Evaluation of the trained NN: (e) the eight raw EMG measurements, and (f) the NN output for detecting the fist posture. The time episodes of different postures can be seen in (f).

have been applied in the pre-processing step. The Z-transform of the filters are $\frac{0.01}{(z-0.99)}$ and $\frac{0.002}{(z-0.998)}$, when the sampling frequency is $1KHz$. The first filter provides short-term memory for the posture identification procedure and the second filter provides longer-term memory. As a result, 24 signals (8 raw plus 16 filtered signals) are considered to find the mentioned mapping. A feed-forward NN is utilized that is composed of three hidden layers. The first and the third layers have 5 perceptrons and the second layer has 15 perceptrons. A linear transfer function is considered for the first and third layers while a log-sigmoid function is considered for the second layer. The training algorithm is Levenberg-Marquardt. A schematic of the NN and the inputs and outputs are shown in Fig. 3(d). To represent the functionality of the proposed procedure, the result for one arm is discussed below when after eleven iterations, the NN converges to the mean-square error of 0.0001. After training the NN, its performance is evaluated for various postures including a new one (i.e., arm pronation-supination). The results are shown in Figs. 3(e) and 3(f) where the raw EMG measurement is given in Fig. 3(e) and the output of the trained NN is given in Fig. 3(f). As can be seen in the figures, the trained NN is capable of detecting the fist posture and distinguishing it from other postures. It should be noted that any other tool that can be trained and used to accurately and in real-time detect and distinguish the posture of interest based on the EMG data can be used as the "EMG Analyzer" in place of the tool explained in this step.●

Step #3) The third step is denoted as *EIST-based Therapy Production*. The main purpose of this step is to map the detected posture of interest to an intended therapeutic behavior for applying various forces and tuning the therapy's strategy and intensity. In other words, this step maps the identified posture of interest to a kinesthetic stimulus, which will then be delivered to the patient's hand by the robot. For this purpose, first the following dynamics are defined:

$$E_{th}(n) = \underset{[-E_m,\, E_m]}{\mathrm{Sat}}\left\{ \eta \cdot \varepsilon_{th}(n) \right\}, \quad where$$

$$\varepsilon_{th}(n) = \alpha \cdot \varepsilon_{th}(n-1) + \beta\left(EMG_{NR}(n) - EMG_{NL}(n) \right)$$

The dynamics given by (8) define the position error $E_{th}(t)$ to be delivered through the viscoelastic constraint in the proposed VR environment (please refer to (7) for definition of position error and the resulting force). In (8), Sat$\{\cdot\}$ is the saturation function whose limits are $[-E_m,\, E_m]$, and n represents the time samples. In addition, η is a scaling factor for normalization to cover the range of position error to be used in the VR environment. Also, $EMG_{NR}(n)$ is the output of the NN trained for the right arm, and $EMG_{NL}(n)$ is the output of the NN trained for the left arm. Accordingly, $(EMG_{NR}(n) - EMG_{NL}(n))$ is termed *differential muscle activity factor* provided by the therapist. Let us initially assume $\alpha = \beta = 1$. The functionality of α and β is explained latter. Based on the above definitions, the therapeutic force generated by the EIST platform is

$$F_{th}(s) = (K_v + \theta_v\, s)\Xi_{th}(s), \quad where\ \Xi_{th}(s) = \mathscr{L}[E_{th}(t)]. \quad (9)$$

In other words, using (8), in order to generate the supervised therapeutic forces, the therapist can tune the position of the

object (corresponding to his/her motion) in the VR environment (like the yellow circle of the shared VR shown in Fig. 2) through providing various formats of posture of interest for his/her right and left arms. In this way, the therapist can tune the intensity and strategy of therapy based on his/her intention. As a result, the patient will feel the kinesthetic forces generated by the virtual viscoelastic constraint, which is stimulated through the existence of $E(t)$. Accordingly, positive values for $E(t)$ result in generation of assistive therapeutic forces and negative values for $E(t)$ result in resistive forces. Here, the position of the therapist in the VR is calculated as

$$p_{th}(t) = p_p(t) + E_{th}(t) \cdot Q(t)$$
$$\text{where} \quad Q(t) = \left(\frac{p_p(t) - p_T(t)}{\|p_p(t) - p_T(t)\|_2} \right). \tag{10}$$

In (10), $p_p(t)$ is the position of the patient, $E_{th}(t)$ is the position error generated by the therapist to provide therapeutic forces through the viscoelastic constraint, $p_T(t)$ is the position of the target, and $Q(t)$ is the normalized unit vector that connects the position of the patient to the one for the target.

Note that in (8), E_m is a positive value considered to provide the maximum and minimum limits for delivery of the position error by the therapist. This can be tuned based on the size of the robot's workspace. The right and left arms of the therapist are considered to identify his/her intention for delivering assistance and resistance, respectively. As a result, considering (8), when the output of the NN trained for detecting the therapist's right fist increases, the $E(t)$ will gradually increase. When the output of the NN trained for detecting the therapist's left fist increases, the $E(t)$ will gradually decrease. Continuous reduction in $E(t)$ value can make it negative. As a result, the therapist is able to tune the intensity and strategy of therapy by providing various formats of posture of interest (in terms of timing of initiation together with the duration of keeping the posture) in left and right arms. ●

Remark 4. Parameter α works like a forgetting factor and should be chosen as $0 \leq \alpha \leq 1$. As a result, if $\alpha = 0$, no memory is considered for the generated therapeutic behavior. This means that once the therapist provides the posture of interest, the resulting position error in the VR will change correspondingly and when the therapist stops the posture, the position error in the VR will become zero. As a result, the therapist needs to keep the posture to deliver the intended therapeutic forces. However, for $\alpha = 1$ the therapist can provide the intended therapy through a "pumping-like" motion. Once the therapist provides the posture of interest, a position error will be set for the patient even if the therapist relaxes his/her hand. The therapist can still decrease/increase the position error using his/her arm postures. As a result, the therapist can "pump-in" and "pump-out" the position error. An α value close (but not equal) to unity results in a similar behavior for the system; however, it introduces a leakage of error in the VR environment. As a result, if the therapist stops providing the posture, the position error will *gradually* converge to zero. The leakage rate correlates with the choice of α (the lower the α value, the faster will be the leakage). This can help the therapist in tuning the required assistance/resistance. ●

Remark 5. Parameter β works like a responsiveness factor that increases the sensitivity to the differential muscle activity
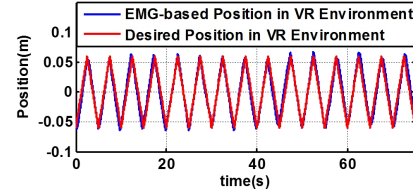
Fig. 4. EMG-based motion tracking in the VR environment.

provided by the therapist. The higher this parameter, the faster the position error will grow in response to $(EMG_{NR}(n) - EMG_{NL}(n))$. By increasing this parameter, the therapist can quickly change the strategy and intensity of the intended therapy while providing less differential muscle activity. α and β are also useful for novice therapists who are not familiar with the operation of this system. As a result, lower values of β provide more control since it reduces the sensitivity; also lower values of α enhance the forgetting feature so that an erroneous input from the therapist will be forgotten even if the therapist does not correct it. ●

To evaluate the behavior of the design proposed in (9), the following experiment was conducted. The user was required to follow a desired trajectory of an object in the VR environment. The trajectory was a periodic triangle wave signal with a frequency of $0.2Hz$ and an amplitude of 6 cm. The user was required to perform the task by tuning the differential muscle activity. The goal was (a) to show that using the proposed EIST platform it is possible to accurately provide varying position trajectory in the VR environment, and (b) to find default values for α and β which result in an appropriate control of the therapy. The results are shown in Fig. 4, where the solid red line shows the required trajectory and the solid blue line shows the position generated by the user. The chosen default values for α and β are 0.999 and 0.1, respectively. As can be seen in Fig. 4, the user was capable of accurately tracking the corresponding position of the moving object in the VR environment. It should be noted that in practical situations, the therapist usually does not change the strategy (which corresponds to the sign of the trajectory) and intensity (which corresponds to the amplitude) as frequently. Here, we showed that using this new platform it is possible to map the intention of the user to track the required behavior in the VR environment through providing differential muscle activities. This can then be used for tuning the intensity and strategy of the intended therapy (as explained before).

Remark 6. It should be noted that in both platforms, increasing the stiffness and viscosity of the coupling reduces the position-dependent and velocity-dependent error between the motions of the therapist's and the one allowed for the patient. The stronger the viscoelastic coupling, the less freedom will be provided for the patient. The amount of θ_v and K_v are fixed and should be defined by the therapist in the first session of therapy, taking into account the performance of the patient. We have demonstrated the system for a group of therapists and based on our observation θ_v value of 20 N.s/m and K_v value of 100 N/m can be considered as default. ●

Remark 7. It should be also noted that for the EIST platform, there is no need for accurate placement of the armbands or for a biomechanical model for the musculoskeletal system of the therapist arms, because (a) an array of the EMG

measurements (collected by the armbands) is used, and (b) a NN-based posture identification is implemented (which is a black-box modeling scheme). ●

B. Phase B: Regeneration Through Modeling

During the second phase of the proposed framework, first the behavior of the therapist, which is registered during the first phase (using either the EIST or HTST platform) in connection with adjusting the strategy and the intensity is modeled in the workspace of the therapy. Then, the modeled therapeutic behavior is regenerated for the patient when the therapist is not engaged. The therapist can assign a duration for therapy regeneration through the RTM phase so that she/he can work with another patient. In summary, during the second phase, the framework *learns* the behavior of the therapist, then *regenerate* the learned behavior during a specific amount of time. In this way, the therapist does not need to spend all of his/her time with one patient and can share it between several patients. This addresses an essential need of under-resourced healthcare systems. In addition, this allows the therapist to intuitively tune the therapy delivered by an HRR system. The second phase is composed of the following two steps.

STEP 1) The first step is to model the therapeutic behavior delivered by the therapist whose corresponding data is logged during the first phase. For this purpose, first, the distribution of the therapeutic position error delivered over the workspace by the therapist is calculated. The distribution represents the therapist's intention in tuning the strategy and intensity of the therapy. Then, the calculated distribution is fed to the *therapy modeling* module. The module is responsible for fitting an NN representation of the therapy, which can be saved and used in the second step where the therapeutic behavior is regenerated. The NN used in this part is composed of three hidden layers where the first and the third layers have 5 perceptrons and the second layer has 15 perceptrons. A linear transfer function is considered for the first and the third layers while a log-sigmoid function is considered for the second layer. The training algorithm is Levenberg-Marquardt. It should be noted that the output of the NN over the workspace of the therapy can be graphically plotted as a *heat map*. The plot is denoted as *Therapeutic Intensity Map (TIM)*. This can be used as a graphical representation of the therapy in follow-up sessions, which intuitively informs the therapist about the therapeutic behavior delivered in the last session. Comparing several TIMs of consecutive sessions can be a useful tool for therapists to monitor the progress of motor performance. In Section IV, examples of the TIM are shown. ●

STEP 2) The second step is when the modeled therapeutic behavior is regenerated and generalized in the workspace of therapy for the patient. The therapist can leave the patient to repetitively perform various rehabilitation tasks. During this step, the trained NN will be utilized to map the current position of the patient in the workspace of therapy to the modeled therapeutic intensity and strategy delivered by the therapist during the first phase. For example, if during the first phase, the therapist provided higher intensity of assistive therapy in parts of the workspace (that can be due to high muscle tone of the patient in that area), the patient will feel more assistive forces

(during the second phase) when her/his motion trajectories pass through that area. Consequently, the input to the trained NN is the current position of the patient in the workspace of the therapy and the output is a therapeutic position error with respect to the target needed to regenerate the required therapeutic intensity and the resulting forces (using (9)). ●

Remark 8. It should be mentioned that to choose the parameters of the neural networks (number of layers and perceptrons), we have conducted several experiments starting from simpler architectures. The reported architecture is a feed-forward NN composed of three hidden layers where the first and the third layers have 5 perceptrons and the second layer has 15 perceptrons. A linear transfer function is considered for the first and third layers while a log-sigmoid function is considered for the second layer. The training algorithm is Levenberg-Marquardt. This architecture provided accurate and consistent results and addressed the main goals. Further modification of the architecture based on patient-based clinical evaluations is part of our ongoing research. ●

IV. RESULTS

In this section, experimental results are given in support of the proposed framework. For this purpose, both HTST and EIST platforms are implemented and tested. The software is implemented on a 64 bit Windows machine. The robots and the NN are run in MATLAB/Simulink using the QUARC 2.2 real-time environment which is provided by the industrial partner of this work QUANSER (Markham, ON, Canada). The VR environment was developed in C++ and communicates with MATLAB through the UDP protocol. In addition, a code developed in C++, reads the raw EMG data and send it through a UDP protocol to MATLAB. The following steps are implemented to conduct the validation.

A. Virtual Reality Environment and the Task

The VR environment is shown in Fig. 2. Also, the corresponding workspace of the robot is shown in Fig. 1(b), where the possible positions of the target are the blue stars and the home position is the red star. The target randomly switches its location in a sequence with a homing motion after each switch. An example of the sequence is [Location #1-Home-Location #4-Location #7-Home-...]. The allowed time for each home-to-target or target-to-home movement was 3 seconds. The target switches its position if (a) the elapsed time for each motion exceeded the 3-second window, or (b) the target was reached within the time window. The definition of reaching was to have a targeting error (Euclidean distance) less than 0.5 *cm*.

B. Simulating Post-stroke and Healthy Users

To provide a comparable and consistent evaluation, motor behaviors of a healthy user and a stroke patient were simulated for the robot. The simulated patient was then assisted using

 (a) Therapist-In-the-Loop HTST scheme (TIL-HTST),
 (b) Therapist-In-the-Loop EIST scheme (TIL-EIST),
 (c) NN trained by the HTST scheme (NN-HTST),
 (d) NN trained by the EIST scheme (NN-EIST).

In general, computational models of the stroke-related deficits can allow researchers to design and analyze the performance

of systems implemented to help post-stroke patients before starting clinical trials [28]. Particularly, in this work, the simulated model allows us to evaluate different features of the platforms under *similar conditions*. For this, the patient-side robot was programmed to conduct the tracking tasks in the VR environment using two different control capabilities (one corresponding to the simulated healthy user and the other corresponding to the simulated disabled user).

To simulate the behavior of a healthy user, a finely tuned classical optimal trajectory controller was implemented which enabled the robot to track the targets within the 3-second window. To simulate the behavior of a post-stroke patient who (a) has imbalanced high muscle tone (hypertonia) due to the stroke and (b) cannot provide enough controlling force to track the target, the following steps were conducted:

1) First, the control gains of the above-mentioned trajectory controller considered for tracking the target was reduced by 70%. This was done since stroke patients usually represent weak control forces to track an object.

2) Second, to simulate the high muscle tone, a nonlinear viscous force field was generated in the workspace, as shown in Fig. 5(a). The post-stroke high tone in muscles usually restricts movement in one direction or parts of the workspace. This concept is used to simulate the imbalanced tone through the viscous force field.

In the next step, the tracking task in the VR environment was conducted by the simulated healthy user and stroke patient during two 5-minute experiments. The results can be seen in Fig. 5. As shown in Figs. 5(b) and 5(d), the simulated healthy user was capable of tracking the target in various parts of the workspace, the task was completed properly, the workspace was covered and the user was capable of reaching all the targets within the 3-second window for each motion.

In contrast, for the simulated post-stroke patient, the trajectories were not properly tracked. This can be seen in Figs. 5(c) and 5(e). In the right side of the workspace ($X \geq 0$), the length of the trajectories were considerably reduced and none of the 5 targets in that region were reached. This was due to the existence of the modeled high muscle tone in that region ($X \geq 0$). In addition, in the left half side of the workspace ($X < 0$), although the trajectories were larger than the right side, still the patient was not able to reach two of the targets within the 3-second window; in addition, there was high lateral deviation, which was due to the poor control capability of the simulated patient. In summary, the simulated patient was not capable of accurately performing the assigned task.

After confirming that, the simulated patient has poor tracking performance in comparison with the simulated healthy user, the next step was to evaluate the performance of the defined four schemes (TIL-HTST, TIL-EIST, NN-HTST, NN-EIST) under similar conditions.

C. Evaluation of the HTST Platform

As mentioned earlier, using the proposed HTST platform, we can deliver direct kinesthetic supervision of a human therapist for a stroke patient. In this part, the performance of the TIL-HTST platform is shown. For this purpose, a human operator used the HD^2 haptic device (therapist-side robot in
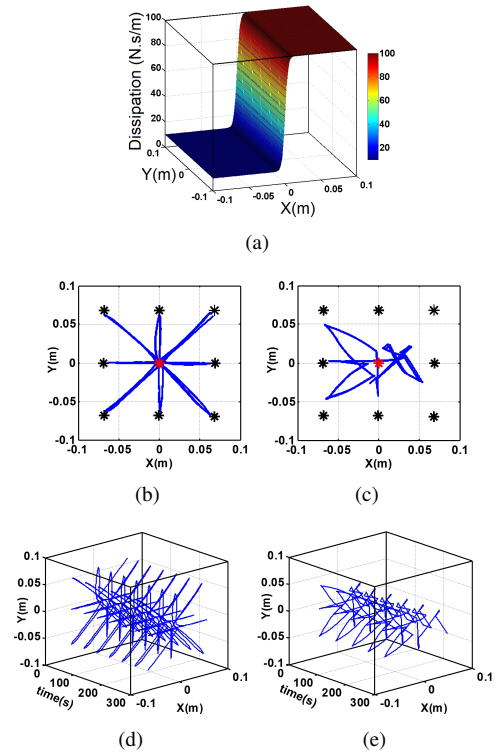
Fig. 5. (a) Generated viscous force field; (b) The modeled healthy user (the resulting overlaid 2D path for task performance); (c) The modeled post-stroke patient (overlaid 2D path); (d) The modeled healthy user (trajectory over time); (e) The modeled post-stroke patient (trajectory over time).

the implemented HTST platform) to provide therapeutic forces in order to recover the target tracking performance of the modeled stroke patient. Figs. 6(a) and 6(b) show the recovered path in 2D and the motion trajectory over time respectively. The experiment was conducted for 5 minutes.

As can be seen in Fig 6, using the implemented HTST platform, the operator was capable of delivering kinesthetic assistance that resulted in rectifying the motion trajectories of the simulated patient. Consequently, using the TIL-HTST platform, the operator playing the role of the therapist provided variable coordinative assistive forces to overcome the reduced control power of the modeled patient and the increased tone in the right side. The information in this stage is logged and is utilized in the next section to train the NN, which can learn and model the assistive behavior of the therapist.

D. Neural Network Training and Therapy Regeneration based on the HTST Platform

The information logged during rehabilitation using the HTST platform was utilized to train a NN. Training of the NN converged (mean square error of 0.00023) after 8 iterations, using Levenberg-Marquardt technique. In this part, the performance of the trained NN is validated. For this purpose, the trained NN is used to generate therapeutic forces for the simulated stroke patient in order to recover the degraded motion control performance. The result of trajectory tracking is shown in Figs. 7(a) and 7(b). As can be seen in Figs. 7(a) and 7(b), the trained NN was capable of properly delivering the required therapy to rectify the trajectories affected by the modeled stroke. As a result, the size of the trajectories on the right side of the workspace is recovered, all the targets are reached and the deviations are reduced. the trained NN
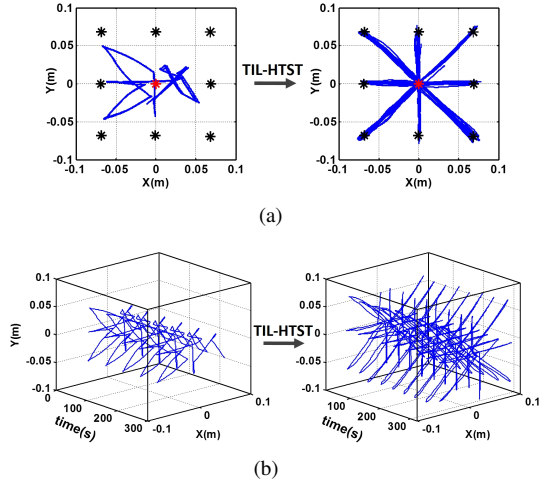
Fig. 6. The capability of the HTST platform in recovering the motion of the modeled stroke patient: (a) overlaid 2D path, (b) trajectory over time.
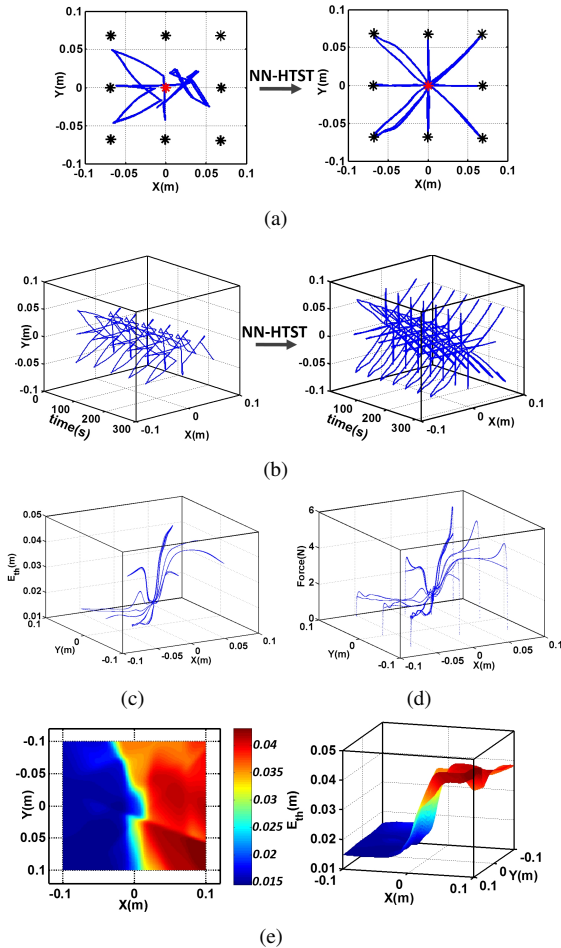
Fig. 7. The capability of the NN-HTST scheme in recovering the motion of the modeled stroke patient: (a) overlaid 2D path, (b) trajectory over time. (c) The position error and (d) the therapeutic forces, generated by the NN trained to deliver therapy based on the logged behavior of the therapist during TIL-HTST trial. (e) The resulting heat map of the therapy using NN-HTST.

was capable of regenerating and generalizing the kinesthetic behavior of the therapist to help the patient's motion tracking capability using no direct information about the characteristics of the simulated patient and by only utilizing information collected during the TIL-HTST trial. The therapeutic position error created by the NN and the corresponding therapeutic

force profile can be seen in Figs. 7(c) and 7(d) respectively. As can be seen in Figs. 7(c) and 7(d), in the right side of the workspace ($X \geq 0$) where the simulated patient showed high muscle tone, the provided therapeutic position error and the corresponding forces were considerably higher.

As mentioned earlier, the trained NN can be evaluated at different points of the workspace and the result can be plotted as a heat map that shows the intensity of the trained therapy. The resulting map encapsulates information regarding the level of infirmity and reduced capability of the patient based on the behavior of the therapist during the TIL-HTST trial. The clinician can use the resulting heat map as a new image modality to evaluate the disability of the patient and analyze improvement by comparing the heat map of consecutive sessions. The resulting heat map of the conducted experiment is shown in Fig. 7(e). Interestingly, the heat map is in agreement with the simulated level of disability. As mentioned before, the simulated patient has high muscle tone on the right side of the workspace which results in reduced tracking capability in that region. This can also be interpreted from Fig. 7(e) which shows that the intensity of the trained therapy delivered on the right side is higher than the one delivered on the left.

E. Evaluation of the EIST Platform

In this subsection, the performance of the proposed TIL-EIST platform is shown. For this purpose, a human operator playing the role of a therapist used the implemented EIST platform to provide therapeutic forces in order to recover the target tracking performance of the modeled stroke patient. Figs. 8(a) and 8(b) show the recovered path in 2D and the motion trajectory over time, respectively. The experiment was conducted for 5 minutes. As can be seen in Fig 8, using the implemented EIST platform, the operator playing the role of the therapist was capable of delivering kinesthetic assistance that resulted in rectifying the motion trajectories of the simulated patient. Consequently, using the TIL-EIST platform the operator provided variable coordinating forces to overcome the reduced control power of the modeled patient and the increased tone in the right side of the workspace. The information in this stage was logged and is used in the next section to train the second NN that can learn the therapeutic behavior delivered by TIL-EIST.

F. NN Training and Therapy Regeneration Based on the EIST

The information logged during rehabilitation using the EIST platform was utilized to train the second NN. Training of the NN converged (mean square error of 0.00029) after 10 iterations, using Levenberg-Marquardt technique. In this part, the performance of the trained NN is validated. For this purpose, the trained NN is used to generate therapeutic forces for the simulated stroke patient in order to recover the degraded motion control performance. The result of trajectory tracking can be found in Figs. 9(a) and 9(b).

As can be seen in the figure, the trained NN was capable of properly delivering the required therapy to recover the trajectories affected by the modeled stroke. As a result, the size of the trajectories on the right side was rectified, all the targets were reached and the deviations were reduced. In other words,
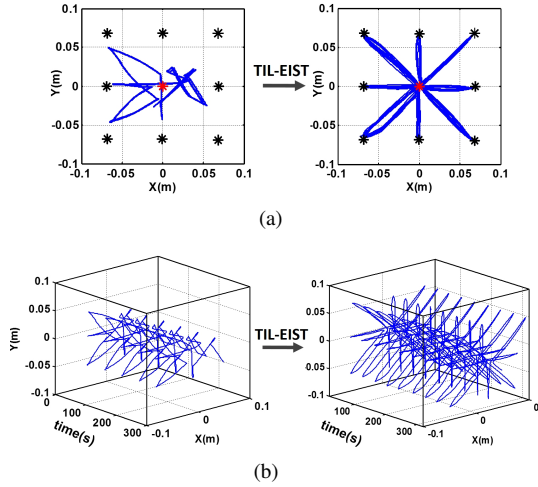
Fig. 8. The capability of the EIST platform in recovering the motion of the modeled post-stroke patient: (a) overlaid 2D path, (b) trajectory over time.

the trained NN was capable of reproducing the behavior of the therapist to recover the tracking performance without any direct information about the characteristics of the simulated patient and by only using information collected during the TIL-EIST trial. The generated therapeutic position error in the VR environment and the corresponding therapeutic force profile are shown in Figs. 9(c) and 9(d).

As can be seen in Figs. 9(c) and 9(d), in the right side of the workspace ($X \geq 0$) where the simulated patient showed high muscle tone and less control capability, the provided therapeutic position error and the corresponding forces were considerably higher. The designed NN based on the EIST platform was also utilized to find the therapeutic heat map. The generated map is shown in Fig. 9(e). The resulting map encapsulates information regarding the level of infirmity and reduced capability based on the behavior of the therapist during the TIL-EIST trial. Similar to the case of the HTST-based map, the map shown in Fig. 9(e) also matches the simulated level of disability.

Based on the results shown in this section, both EIST and HTST platforms were capable of delivering TIL robotic rehabilitation. The information logged during therapy delivery by the proposed platforms can be utilized to train neural networks to regenerate the same therapeutic behavior while the therapist is outside of the therapy loop. The proposed training technique can encapsulate the rehabilitative preference of a skilled human therapist for delivering kinesthetic therapy and can fill the gap between conventional HRR systems and standard therapist-in-the-loop hand-over-hand therapy.

V. CONCLUSION

In this paper, a new framework was proposed to tune the intensity and strategy of haptic rehabilitation systems based on the registered kinesthetic supervision of a therapist. The proposed framework has two phases, namely: Supervised Therapy Demonstration (STD) and Regeneration through Modeling (RTM). Two platforms were considered as alternatives which can register a therapist's intention for modifying the therapy during the STD phase. The platforms were denoted by (a)
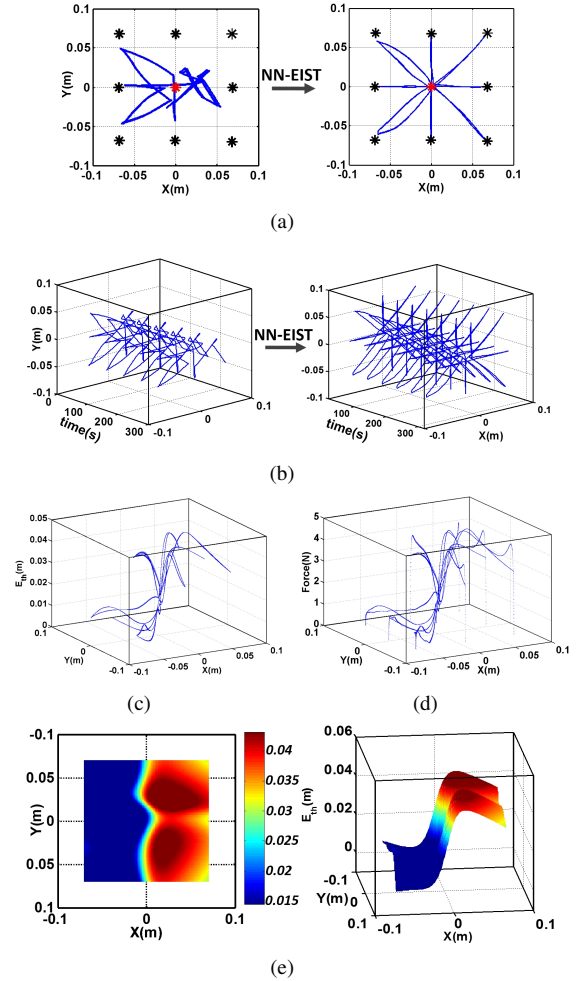
Fig. 9. The capability of the NN-EIST scheme in recovering the motion of the modeled stroke patient: (a) overlaid 2D path, (b) trajectory over time. (c) The position error and (d) therapeutic forces, generated by the NN trained to deliver therapy based on the logged behavior of the therapist during the TIL-EIST trial. (e) The resulting heat map of the therapy using NN-EIST.

Haptics-enabled Teleoperated Supervised Training (HTST) and (b) EMG-based Indirect Supervised Training (EIST). Although in contrast to the EIST platform (proposed in this paper), the HTST platform can provided *direct* haptic awareness for the therapist (during the STD phase), the EIST platform is safer to operate, portable and more cost-effective. Both platforms are capable of (a) realizing kinesthetic supervision of a therapist for robotic therapy, and (b) providing the therapist with some degree of haptic awareness. During the RTM phase, the registered therapeutic behavior of the therapist is modeled using a neural network that can then regenerate the behavior for the patient. As a result, a therapist can demonstrate a brief session of kinesthetic robotic therapy; then the therapist can set a length of time for the patient to independently practice based on the modeled behavior. This saves the therapist's time, which is an important benefit to under-resourced healthcare systems. In this paper, the engineering design of the platform was presented. It should be noted that the flexible NN-based design of the proposed framework allows for further extension of the technique and considering several other features and factors which have not been considered at this stage. Further analysis of this will form part of our future work. In the experiments, an end-point robotic system was utilized, which was developed by

our industrial partner, Quanser Inc. (Markham, ON, Canada). In this paper, we used position-based therapeutic tasks. To the best of our knowledge, this paper reports one of the earliest designs and implementations of a AI-based learning-from-demonstration strategy for training of rehabilitation robots under the kinesthetic supervision of a therapist. Our future work will focus on patient-based studies of the proposed technology and clinical experiments of the technique. This paper does not concern about delay-related stability issues. Discussions about the effects of delay on telerobotic systems can be found in the literature such as [29], [30], [31], [27].

REFERENCES

[1] M. J. Johnson, *et al.*, "Collaborative tele-rehabilitation and robot-mediated therapy for stroke rehabilitation at home or clinic," *Intelligent Service Robotics*, vol. 1, no. 2, pp. 109–121, Apr 2008.

[2] H. I. Krebs and N. Hogan, "Therapeutic robotics: A technology push," *Proceedings of the IEEE*, vol. 94, no. 9, pp. 1727–1738, 2006.

[3] M. Molinari, *et al.*, "Rehabilitation technologies application in stroke and traumatic brain injury patients," in *Emerging Therapies in Neurorehabilitation II*. Springer, 2016, pp. 29–64.

[4] N. C. Bejarano, *et al.*, "Robot-assisted rehabilitation therapy: Recovery mechanisms and their implications for machine design," in *Emerging Therapies in Neurorehabilitation II*. Springer, 2016, pp. 197–223.

[5] L. Masia, *et al.*, "Design and characterization of hand module for whole-arm rehabilitation following stroke," *IEEE/ASME Transactions on Mechatronics*, vol. 12, no. 4, pp. 399–407, Aug 2007.

[6] N. Hogan, *et al.*, "Motions or muscles? some behavioral factors underlying robotic assistance of motor recovery," *Journal of Rehabilitation Research and Development*, vol. 43, no. 5, pp. 605–618, 2006.

[7] R. Sigrist, *et al.*, "Augmented visual, auditory, haptic, and multimodal feedback in motor learning: A review," *Psychonomic Bulletin & Review*, vol. 20, no. 1, pp. 21–53, 2013.

[8] L. Marchal-Crespo and D. J. Reinkensmeyer, "Review of control strategies for robotic movement training after neurologic injury," *Journal of Neuroengineering and Rehabilitation*, vol. 6, no. 1, p. 20, 2009.

[9] M. Shahbazi, *et al.*, "Robotics-assisted mirror rehabilitation therapy: A therapist-in-the-loop assist-as-needed architecture," *IEEE/ASME Transactions on Mechatronics*, vol. 21, no. 4, pp. 1954–1965, Aug 2016.

[10] A. U. Pehlivan, *et al.*, "A subject-adaptive controller for wrist robotic rehabilitation," *IEEE/ASME Transactions on Mechatronics*, vol. 20, no. 3, pp. 1338–1350, June 2015.

[11] J. Hidler, *et al.*, "Multicenter randomized clinical trial evaluating the effectiveness of the lokomat in subacute stroke," *Neurorehabilitation and Neural Repair*, vol. 23, no. 1, pp. 5–13, 2009.

[12] T. G. Hornby, *et al.*, "Enhanced gait-related improvements after therapist-versus robotic-assisted locomotor training in subjects with chronic stroke a randomized controlled study," *Stroke*, vol. 39, no. 6, pp. 1786–1792, 2008.

[13] O. Barzilay and A. Wolf, "Adaptive rehabilitation games," *J of Electromyography and Kinesiology*, vol. 23, no. 1, pp. 182 – 189, 2013.

[14] A. G. Billard, *et al.*, "Learning from humans," in *Springer Handbook of Robotics*. Springer, 2016, pp. 1995–2014.

[15] L. Rozo, *et al.*, "Learning physical collaborative robot behaviors from human demonstrations," *IEEE Transactions on Robotics*, vol. 32, no. 3, pp. 513–527, June 2016.

[16] B. Huang, *et al.*, "A modular approach to learning manipulation strategies from human demonstration," *Autonomous Robots*, vol. 40, no. 5, pp. 903–927, 2016.

[17] L. Rozo, *et al.*, "A robot learning from demonstration framework to perform force-based manipulation tasks," *Intelligent service robotics*, vol. 6, no. 1, pp. 33–51, 2013.

[18] A. Kucukyilmaz and Y. Demiris, "One-shot assistance estimation from expert demonstrations for a shared control wheelchair system," in *Robot and Human Interactive Communication (RO-MAN), 2015 24th IEEE International Symposium on*, Aug 2015, pp. 438–443.

[19] H. Soh and Y. Demiris, "Learning assistance by demonstration: Smart mobility with shared control and paired haptic controllers," *Journal of Human-Robot Interaction*, vol. 4, no. 3, pp. 76–100, 2015.

[20] M. Maaref, *et al.*, "A gaussian mixture framework for co-operative rehabilitation therapy in assistive impedance-based tasks," *IEEE Journal of Selected Topics in Signal Processing*, vol. 10, no. 5, pp. 904–913, 2016.

[21] S. F. Atashzar, *et al.*, "A small-gain approach for nonpassive bilateral telerobotic rehabilitation: Stability analysis and controller synthesis," *IEEE Transactions on Robotics*, vol. 33, no. 1, pp. 49–66, Feb 2017.

[22] S. F. Atashzar, *et al.*, "A passivity-based approach for stable patient-robot interaction in haptics-enabled rehabilitation systems: Modulated time-domain passivity control," *IEEE Transactions on Control Systems Technology*, vol. 25, no. 3, pp. 991–1006, May 2017.

[23] S. F. Atashzar, *et al.*, "Networked teleoperation with non-passive environment: Application to tele-rehabilitation," in *IEEE/RSJ International Conference on Intelligent Robots and Systems*, 2012, pp. 5125–5130.

[24] S. F. Atashzar, *et al.*, "Projection-based force reflection algorithms for teleoperated rehabilitation therapy," in *IEEE/RSJ International Conference on Intelligent Robots and Systems*, 2013, pp. 477–482.

[25] C. Pacchierotti, *et al.*, "Cutaneous feedback of fingertip deformation and vibration for palpation in robotic surgery," *IEEE Transactions on Biomedical Engineering*, vol. 63, no. 2, pp. 278–287, Feb 2016.

[26] M. Kitagawa, *et al.*, "Effect of sensory substitution on suture-manipulation forces for robotic surgical systems," *The Journal of thoracic and cardiovascular surgery*, vol. 129, no. 1, pp. 151–158, 2005.

[27] S. F. Atashzar, *et al.*, "A grasp-based passivity signature for haptics-enabled human-robot interaction: Application to design of a new safety mechanism for robotic rehabilitation," *The International Journal of Robotics Research*, vol. 36, no. 5-7, pp. 778–799, 2017.

[28] S. M. Sketch, *et al.*, "Simulating the impact of sensorimotor deficits on reaching performance," in *2017 International Conference on Rehabilitation Robotics (ICORR)*, July 2017, pp. 31–37.

[29] P. F. Hokayem and M. W. Spong, "Bilateral teleoperation: An historical survey," *Automatica*, vol. 42, no. 12, pp. 2035–2057, 2006.

[30] G. Niemeyer and J. Slotine, "Telemanipulation with time delays," *The International Journal of Robotics Research*, vol. 23, pp. 873–890, 2004.

[31] Z. Chen, *et al.*, "Integrated adaptive robust control for multilateral teleoperation systems under arbitrary time delays," *International Journal of Robust and Nonlinear Control*, vol. 26, no. 12, pp. 2708–2728, 2016.

S. Farokh Atashzar (S'11-M'17) obtained his Ph.D. degree in Electrical and Computer Engineering (ECE) from the University of Western Ontario (UWO), Canada, in 2016. Currently, he is a postdoctoral research associate in Rehabilitation Engineering and Assistive Control Technologies (REACT) lab at UWO, and Canadian Surgical Technologies and Advanced Robotics (CSTAR). He was a visiting research scholar at the University of Alberta, Canada, in 2014. His research broadly involves areas of medical robotics, physical human-robot interaction, bio-signal processing, machine learning, and advanced control systems.

Mahya Shahbazi (S'10-M'17) received the Ph.D. degree in ECE from UWO, in January 2017. She is currently a Postdoctoral Research Associate with the Department of Electrical and Computer Engineering at UWO and CSTAR. She was a Visiting Research Scholar at the University of Alberta, Edmonton, AB, Canada. Her research interests include medical robotics, telerobotics, humanrobot interaction, artificial intelligence, and advanced control systems.

Mahdi Tavakoli (M'08) is a Professor in the Dept. of Electrical and Computer Engineering, University of Alberta, Canada. He received his PhD degree from UWO, Canada, in 2005. In 2006, he was a post-doctoral researcher at CSTAR. In 2007-2008, he was an NSERC Post-Doctoral Fellow at Harvard University, USA. Dr. Tavakolis research interests broadly involve the areas of robotics and systems control. He is currently on the Editorial Board of the Journal of Medical Robotics Research.

Rajni V. Patel (M'76, SM'80, F'92, LF'13) received the PhD degree from the University of Cambridge, England, in 1973. He currently holds the position of Distinguished University Professor and Tier-1 Canada Research Chair in the Dept. of Electrical and Computer Engineering at UWO, Canada. He also serves as Director of Engineering for CSTAR. He has served on the editorial boards of the IEEE Tran. on Robotics, and the IEEE/ASME Tran. on Mechatronics, and is currently on the Editorial Board of the International Journal of Medical Robotics.